Journal of Inorganic Biochemistry 229 (2022) 111726

Contents lists available at ScienceDirect

Journal of Inorganic Biochemistry

journal homepage: www.elsevier.com/locate/jinorgbio

Antileishmanial activity and insights into the mechanisms of action of symmetric Au(I) benzyl and aryl-N-heterocyclic carbenes

Letícia B. Rosa [a], Carolina Galuppo [b], Rochanna L.A. Lima [b], Josielle V. Fontes [b], Fábio S. Siqueira [c], Wagner A.S. Júdice [c], Camilla Abbehausen [b,*], Danilo C. Miguel [a,*]

[a] Department of Animal Biology, Institute of Biology, State University of Campinas – UNICAMP, Campinas, SP, Brazil
[b] Department of Inorganic Chemistry, Institute of Chemistry, State University of Campinas – UNICAMP, Campinas, SP, Brazil
[c] Interdisciplinary Center for Biochemical Research, University of Mogi das Cruzes, Mogi das Cruzes, SP, Brazil

ARTICLE INFO

Keywords:
American Tegumentary Leishmaniasis
Antileishmanial
Au(I)
Leishmania
Metal
N-heterocyclic carbenes

ABSTRACT

Leishmania amazonensis and *L. braziliensis* are the main etiological agents of the American Tegumentary Leishmaniasis (ATL). Taking into account the limited effectiveness and high toxicity of the current drug arsenal to treat ATL, novel options are urgently needed. Inspired by the fact that gold-based compounds are promising candidates for antileishmanial drugs, we studied the biological action of a systematic series of six (1)-(6) symmetric Au(I) benzyl and aryl-N-heterocyclic carbenes. All compounds were active at low micromolar concentrations with 50% effective concentrations ranging from 1.57 to 8.30 μM against *Leishmania* promastigotes. The mesityl derivative (3) proved to be the best candidate from this series, with a selectivity index ~13 against both species. The results suggest an effect of the steric and electronic parameters of the N-substituent in the activity. Intracellular infections were drastically reduced after 24h of (2)-(5) incubation in terms of infection rate and amastigote burden. Further investigations showed that our compounds induced significant parasites' morphological alterations and membrane permeability. Also, (3) and (6) were able to reduce the residual activity of three *Leishmania* recombinant cysteine proteases, known as possible targets for Au(I) complexes. Our promising results open the possibility of exploring gold complexes as leishmanicidal molecules to be further screened in *in vivo* models of infection.

Table of Abbreviations

ATL	American Tegumentary Leishmaniasis
BMDM	bone marrow-derived macrophages
CC_{50}	50% cytotoxic concentration
CP	cysteine protease
DMAP	dimethylaminopyridine
EC_{50}	50% effective concentration
EtBr	ethidium bromide
FBS	fetal bovine serum
NHC	N-heterocyclic carbenes
NMR	nuclear magnetic resonance
NTDs	neglected tropical diseases
rCP	recombinant cysteine protease
SI	selectivity index

1. Introduction

Neglected tropical diseases (NTDs) pose a great burden on more than 1 billion people worldwide especially in poor and developing countries. Leishmaniasis is one of the leading examples of NTDs that affects 0.7 to 1 million people in 98 countries [1,2]. The disease is caused by the intracellular stage of *Leishmania* protozoan parasites known as amastigotes. During its life cycle, *Leishmania* is transmitted by sandflies vectors as extracellular promastigotes that are inoculated in the dermis of the vertebrate host. Mononuclear phagocytic cells will engulf infective promastigotes that encounter favorable conditions to differentiate into amastigotes. The replication and dissemination of these intracellular forms are crucial for the disease establishment. In this case, symptoms vary from spontaneously healing skin lesions to visceral organs impairment depending on the species, geographic location and the immune status of the host [1,3].

In Brazil, American Tegumentary Leishmaniasis (ATL) is caused by

* Corresponding authors.
E-mail addresses: camilla@unicamp.br (C. Abbehausen), dcmiguel@unicamp.br (D.C. Miguel).

https://doi.org/10.1016/j.jinorgbio.2022.111726
Received 8 December 2021; Received in revised form 5 January 2022; Accepted 9 January 2022
Available online 15 January 2022

several species, being *L. braziliensis* the most relevant followed by *L. amazonensis*. ATL presents distinct clinical forms, such as localized, mucocutaneous, disseminated or diffuse leishmaniasis [4]. In all cases, chemotherapeutic options are limited due to long schemes of parenteral administration of very toxic drugs, including pentavalent antimonials, pentamidine, and paromomycin [5].

Considering that the first choice treatment currently used for leishmaniasis is an antimony-based compound, a number of metals have been explored as leishmanicidal agents, such as copper [6], ruthenium [7], palladium [8], among others [9,10]. One of the greatest advantages of metallic compounds is that they may present more than one mode of action, reaching multiple targets or targets that are undruggable by organic compounds. For this reason they show great potential to hamper the selection of resistant parasite strains [11].

In this scenario, Au(I) complexes gained special attention due to its thiophilic feature and its anti-inflammatory, anticancer and antiparasitic activities. These complexes act on a multitude of targets due to the structural diversity of ligands and their resulting complexes, leading to several biological effects, including cell cycle alteration, generation of reactive oxygen species that can lead to mitochondrial and DNA damage, inhibition of cysteine proteases, thioredoxin reductase and topoisomerase IB. The high affinity of gold compounds with selenoproteins and sulfur-rich proteins makes them powerful drug candidates and can interact with important enzymes involved in redox homeostasis in *Leishmania* [11,12].

N-heterocyclic carbenes (NHC) have emerged as potential pharmacological organometallic ligands for metals, especially Au(I), due to its strong σ donor and medium π-acceptor character, decreasing the extent of substitution reactions and promoting the stabilization of oxidation state. NHC are easily modulated, allowing chemical modification to achieve the biological performance required. Sterically hindered and electron donating groups bound to NHC by the nitrogen atoms can promote extra stabilization of the Au(I) compound [13]. On the other hand, additional physical chemical properties such as lipophilic/hydrophilic balance, pH sensitivity, and protein interaction can be fine-tuned by the chemical groups present in the NHC. As recently reviewed by our group, several Au(I)-NHC compounds had their leishmanicidal activity investigated. Most of them focused on asymmetric NHC compounds or cationic bis-carbenes tested in *L. major* or *L. infantum* [11]. Very recently, Minori and colleagues found low EC_{50} values for cationic $[Au^{I}(1\text{-benzyl-}3,7,9\text{-trimethylxanthine-}8\text{-ylidene})_2]BF_4$ against *L. amazonensis and L. braziliensis* and significant decreases of intracellular infection rates [14]. H. Gornitzka's research group has demonstrated low EC_{50} for *L. infantum* axenic amastigotes when testing neutral and cationic asymmetric Au(I)-NHC bearing different functionalization [15,16].

Based on these biological effects induced by Au-complexes, we aimed to evaluate a series of six Au(I) symmetric benzyl or aryl-N-heterocyclic carbenes (1)–(6) to determine their activity against *L. amazonensis* and *L. braziliensis* with insights on potential mechanisms of action. The series was designed to evaluate the effect of the N-benzyl or N-aryl group in the heteroleptic [Au(*I*)Cl(NHC)] compounds by structure/activity understanding. Dimethylaminopyridine (DMAP) was used to design cationic heteroleptic complexes of formula $[Au(I)(DMAP)(NHC)]^{+}$. DMAP was chosen as it has been demonstrated to slow down substitution reactions and increase water solubility as the binding constant with aryl-based amino acids (tryptophan, for example) [17]. Briefly, significant differences in leishmanicidal activity were observed depending on the N-group. Morphological alterations were observed for all compounds and significant differences provide insights on the structure/activity relationship. The best compounds promoted the permeabilization of membrane and inhibition of recombinant *Leishmania* cysteine proteases.

2. Experimental section

2.1. Materials and equipments

All chemicals used in this work were reagent grade. Except for aniline, which was purified according to described methodology [18], all chemicals were used without further purification. Chloro(tetrahydrothiophene)gold(I), [AuCl(tht)] was synthesized according to Uson et al. [19] from potassium tetrachloroaurate and tetrahydrothiophene (tht) (Sigma Aldrich, Brazil). The electrospray ionization mass spectra (ESI-MS) in the positive and negative mode were recorded with a Thermo Q Exactive Orbitrap Mass Spectrometer with Heated Electrospray Ionization (HESI-II) Probe. Solution ^{1}H, and ^{13}C, NMR spectra were acquired on a Bruker Avance III HD 250 MHz, Bruker Avance III 400 MHz or Bruker Avance III 500 MHz multinuclear spectrometer as indicated, using tetramethylsilane as the reference for ^{1}H and ^{13}C NMR.

2.2. Synthesis of compounds

2.2.1. Synthesis of 1,3-diphenyl-1H-imidazolium tetrafluoroborate (IPh·HBF$_4$)

The synthesis of IPh·HBF_4 followed an adapted procedure described by Murer et al. [20]. The product was precipitated from an aqueous solution using NH_4BF_4 instead of HBF_4 described in the original procedure, producing a crystalline light orange powder. ^{1}H NMR (DMSO-d_6, 400 MHz, ppm): 7.67 (m, 2H, pH-p), 7.73 (m, 4H, pH-m), 7.92 (dd, 4H, pH-o), 8.59 (d, 2H, CH═CH, Im), 10.34 (s, 1H, N-CH-N, Im). ESI+ MS (*m/z*, monoisotopic): 221.10694, $[C_{15}H_{13}N_2]^{+}$ (calc. 221.10732). Yield: 27%.

2.2.2. Synthesis of 1,3-dibenzyl-1H-imidazolium tetrafluoroborate (IBn·HBF$_4$)

The synthesis of IBn·HBF_4 was performed according to the procedure described by Moore et al. and Hans et al. [21,22]. ^{1}H NMR ($CDCl_3$, 400 MHz, ppm): 5.31 (s, 4H, CH_2), 7.16 (d, 2H, CH═CH, Im), 7.37 (m, 10H, Ar), 9.11 (s, 1H, N-CH-N, Im). ESI+ MS (*m/z*, monoisotopic): 249.13974, $[C_{17}H_{17}N_2]^{+}$ (calc. 249.13863). Yield: 65%.

2.2.3. Synthesis of 1,3-bis-(2,6-diisopropylphenyl)-1H-imidazolium chloride (IPr·HCl)

The synthesis of IPr·HCl was performed as previously described [21,22]. ^{1}H NMR ($CDCl_3$, 250 MHz, ppm): 1.24 (d, 12H, $CH(CH_3)_2$), 1.29 (d, 12H, $CH(CH_3)_2$), 2.45 (q, 4H, $CH(CH_3)_2$), 7.36 (d, 4H, m-Ar), 7.58 (m, 2H, p-Ar), 8.12 (s, 2H, CH═CH, Im), 9.92 (s, 1H, N-CH-N, Im). ESI+ MS (*m/z*, monoisotopic): 389.29506, $[C_{27}H_{37}N_2]^{+}$ (calc. 389.29513). Yield: 80%.

2.2.4. Synthesis of 1,3-bis-(2,4,6-trimethylphenyl)-1H-imidazolium chloride (IMes·HCl)

The synthesis of IMes·HCl was performed as previously described [21,22]. ^{1}H NMR ($CDCl_3$, 250 MHz, ppm): 2.13 (s, 12H, o-CH_3), 2.36 (s, 6H, p-CH_3), 7.05 (s, 4H, m-CH), 7.57 (s, 2H, CH═CH, Im), 8.89 (s, 1H, N-CH-N, Im). ESI+ MS (*m/z*, monoisotopic): 305.20077, $[C_{21}H_{25}N_2]^{+}$ (calc. 305.20123). Yield: 80%.

2.2.5. Synthesis of [AuCl(IPr)] (1) and [AuCl(IMes)] (3)

The complexes (1) and (3) were synthesized adapting the methodology of Visbal et al. [23]. In round bottom flask [Au(*tht*)Cl] (0.35 mmol, 0.1122 g) and IMes·HCl (0.35 mmol, 0.1193 g) was dissolved in CH_2Cl_2 (15 mL). After 15 min, K_2CO_3 (0.7 mmol, 0.967 g) was added and the reaction was kept under stirring for 1.5 h. The solvent excess was removed in a rotary evaporator, precipitating a solid that was collected by filtration. The solid was purified by recrystallization in dichloromethane at −20 °C for 24 h. The crystals were collected and washed with diethyl ether.

(1) Yield: 41% ^{1}H NMR (500 MHz, CD_3Cl, ppm): 1.24 (dd, 12H, CH

($C\underline{H}_3)_2$), 1.37 (d, 12H, CH($C\underline{H}_3)_2$), 2.57 (m, 4H, C$\underline{H}$($CH_3)_2$), 7.18 (d, 2H, CH═CH, Im), 7.27 (m, 4H, m-Ar, IPr), 7.51 (m, 2H, p-Ar, IPr). ESI+ MS (*m/z*, monoisotopic): 626.27868, $[C_{27}H_{37}N_2Au(CH_3CN)]^+$ (calc. 626.28040).

(3) Yield: 91%. ^{1}H NMR (500 MHz, CD_3Cl, ppm): 2.11 (s, 12H, o-CH_3), 2.35 (s, 6H, p-CH_3), 7.00 (s, 4H, m-Mes), 7.10 (s, 2H, CH═CH, Im). ESI+ MS (*m/z*, monoisotopic): 542.18520, $[C_{21}H_{24}N_2Au(CH_3CN)]^+$ (calc. 542.18650).

2.2.6. Synthesis of [AuCl(IPh)] (2) and [AuCl(IBn)] (4)

The complexes (2) and (4) were prepared according to adapted procedures from Visbal et al. and Collado et al. [23,24]. The respective tetrahydroborate imidazolium (IPh·HBF_4 or IBn·HBF_4, 0.40 mmol), [AuCl(tht)] (0.30 mmol) and tetramethylammonium chloride (2.00 mmol) were dissolved in dichloromethane. The solution was kept under stirring for 30 min at room temperature, followed by addition of potassium carbonate (6.02 mmol). The reaction was kept under stirring at room temperature for 2.5 h. The solid was filtered off over Celite® and the solvent removed under reduced pressure. The white solid was recrystallized in dichloromethane/ether, filtered, washed with ether and dried under reduced pressure.

(2) Yield: 45%. ^{1}H NMR (250 MHz, CD_3Cl, ppm): 7.39 (s, 2H, CH═CH, Im), 7.51–7.59 (m, 6H, CH, m-Ph, p-Ph), 7.72–7.76 (m, 4H, o-Ph). ESI+ MS (*m/z*, monoisotopic): 458.09176, $[C_{15}H_{12}N_2Au(CH_3CN)]^+$ (calc. 458.09260).

(4) Yield: 28%. ^{1}H NMR (500 MHz, CD_3Cl, ppm): 5.40 (s, 4H, CH_2, Bn), 6.87 (s, 2H, CH═CH, Im), 7.32–7.41 (m, 10H, CH, Bn). ESI+ MS (m/z, monoisotopic): 486.12274, $[C_{17}H_{16}N_2Au(CH_3CN)]^+$ (calc. 486.12390).

2.2.7. Synthesis of [au(DMAP)(IBn)]NO_3 (5) and [au(DMAP)(IPr)]NO_3 (6)

The methodology to prepare (5) and (6) were adapted from Abbehausen et al. [17]. In a flask complexes (1) or (4) (1 mmol) were dissolved in sufficient amounts of chloroform. An ethanolic solution containing 1 mmol of $AgNO_3$ was prepared and added to the complex solution, precipitating AgCl which was removed by filtration over Celite® or using a 2 μm syringe filter. To the clear solution of the complex, a chloroform solution of 4-dimethylaminopyridine (DMAP) (1 mmol) was added and left under stirring overnight at room temperature and protected from the light. Then, the solvent was removed under reduced pressure forming a transparent film that was dissolved in acetone and refrigerated to −20 °C, precipitating a crystalline white solid.

(5) Yield: 44%. ^{1}H NMR (500 MHz, CD_3Cl, ppm): 3.13 (s, 6H, CH_3, DMAP), 5.46 (s, CH_2, Bn), 6.69 (d, 2H, m-CH, DMAP), 7.15 (d, 2H, CH═CH, Im), 7.37 (m, 10H, CH, Bn), 7.99 (d, 2H, o-CH, DMAP). ESI+ MS (*m/z*, monoisotopic): 567.17993, $[C_{24}H_{26}N_4Au]^+$ (calc. 567.18175).

(6) Yield: 32%. ($CDCl_3$, 250 MHz, ppm): 1.31 (dd, 24H, CH($C\underline{H}_3)_2$), 2.58 (q, 5H, CH($CH_3)_2$), 3.27 (s, 5.8H, CH_3, DMAP), 6.76 (d, 2.0H, m-CH, DMAP), 7.19 (s, 1.8H, CH═CH, Im), 7.36 (d, 4.1H, m-Ar), 7.53 (t, 2.2H, p-Ar), 8.22 (d, 2.1H, o-CH, DMAP). ESI+ MS (*m/z*, monoisotopic): 707.33528, $[C_{34}H_{46}N_4Au]^+$ (calc. 707.33825).

2.3. Parasites

Leishmania (Leishmania) amazonensis (IFLA/BR/1967/PH8) and *L. (Viannia) braziliensis* (MHOM/BR/1994/H3227) promastigotes were grown at 25 °C in 25 cm^2 tissue culture flasks containing M199 medium (Gibco-Invitrogen) supplemented as described [25]. *L. braziliensis* cultures were supplemented with 2% male sterile human urine and 10% fetal bovine serum (FBS). Cultures were split every 5 days, after promastigotes reach late logarithmic growth phase. Axenic amastigotes of *L. amazonensis* were obtained as previously described [26] and kept in acidified M199 (pH 4.8) for up to two weeks with splits every three days.

2.4. Extraction of primary host cells

Bone marrow-derived macrophages (BMDM) were obtained after differentiation of precursor cells extracted from femurs and tibias of female Balb/C mice. The medullary cavities of the bones were washed with a 5 mL syringe and a 21G needle with Roswell Park Memorial Institute (RPMI 1640) medium (Gibco-Invitrogen) supplemented with 20% FBS and 30% L929 fibroblast culture supernatant in 75 mm Petri dishes. Recovered cells were kept at 37 °C with 5% CO_2 atmosphere. After 7 days, differentiated BMDM were collected with fresh RPMI medium after scraping the plate with a sterile cell scraper (Biofil®) [25]. The Ethics Committee on Animal Use of the University of Campinas (CEUA-UNICAMP) (protocol #5389–1/2019) approved all procedures using mice.

2.5. Cell viability assays

Cell viability was evaluated by the MTT ((3-(4,5-dimethylthiazol-2-yl)-2,5-diphenyltetrazolium bromide) assay [27] using log phase promastigote cultures (5×10^6 cells/well) or BMDM (4×10^5 cells/well) in 96-well culture plates incubated with increasing concentrations of (1) to (6) for 24 h. All Au(I) complexes were freshly solubilized in pure sterile DMSO (Sigma Aldrich) at 25 mM stocks for each experiment. Briefly, 30 μL of MTT (5 mg/mL) was added to each well and the plates were incubated for 2 h at 25 °C (for promastigotes) and 37 °C (for macrophages). Next, the reaction was stopped by addition of 30 μL of SDS 20%. Absorbance reading was performed using a plate spectrophotometer (reference and test wavelength of 690 and 595 nm, respectively). Optical density values were converted to percentages compared to untreated control groups incubated with medium only (100% viability) to determine the 50% effective concentrations (EC_{50} for parasites and CC_{50} for macrophages) from sigmoidal regression of dose-response curves (GraphPad Prism6 software, USA).

2.6. Thick smears for parasite's morphology evaluation

Culture aliquots of 10 μL from cell viability assays were placed on glass slides for thick smears preparation. Next, the smears were dried at room temperature for 24 h, fixed with pure methanol for 1 min and stained with an InstantProv kit (NewProv, Brazil). At least 150 promastigotes were examined for each NHC complex tested by optical microscopy (100× oil immersion, Nikon Eclipse E200, Nikon Corp.). Parasite's morphology were classified as: 'fusiform', 'replicating', 'round', 'aberrant' and 'sperm-like' and the frequency of each form (%) was calculated for each complex-treated and untreated cultures.

2.7. In vitro infection assay

To assess the viability of intracellular amastigotes, 4×10^5 BMDM were cultured per well containing 13 mm glass coverslip in 24-well plates. Next, cells were incubated with stationary phase promastigotes of *L. amazonensis* (5 parasites: 1 macrophage) and *L. braziliensis* (10:1) for 16 h at 34 °C and 5% CO_2 and then exposed or not to increasing concentrations of the gold compounds for 24 h. Coverslips were fixed with pure methanol and stained with an Instant Prov kit (NewProv, Brazil). The number of infected cells and amastigotes per 100 BMDM were quantified microscopically by direct counting as described [14]. Infection rates (%) were determined as the proportion of BMDM containing at least one intracellular parasite in a total of 100 infected and non-infected BMDM. Infectivity indexes (percentage of infected cells *x* amastigote number per infected cell) were also determined.

2.8. Plasma membrane permeability assay

The ability of NHC complexes to interfere with parasite's plasma membrane integrity was assessed using 5×10^6 promastigotes or 1×10^7

amastigotes of *L. amazonensis* incubated with medium only or with EC_{50} or half- EC_{50} of (3) for different time points and exposed to 100 μM bromide (EtBr). Fluorescence signals were recorded using a HITACHI F2500 fluorimeter (excitation at 365 and emission at 580 nm). Maximum peaks of EtBr incorporation were obtained after the addition of 1.6 mM of digitonin [14].

2.9. Inhibitory activity of recombinant CPBs

The enzymes (rCPB2.8, rCPB3.0 and rH84Y) were expressed and purified at the Interdisciplinary Center for Biochemical Research, according to [28]. The final concentration of each enzyme was 15 nM. Enzymatic assays using *L. mexicana* recombinant CPBs (rCPB2.8, rCPB3.0 and rH84Y) were performed using 100 mM sodium acetate buffer, 20% glycerol, 0.01% Triton X-100, 5 mM DTT (1,4-dithiothreitol) (pH 5.5) with enzyme preactivation for 5 min at 37 °C under constant agitation in a quartz cuvette with 1 mL final volume. The enzymatic activities were monitored in a spectrofluorometer (F2700; Hitachi, Japan) and the hydrolysis of Z-FR-MCA (carbobenzoxy-Phe-Arg-7-amide-4-methylcoumarin) substrate (Bachem, USA) was monitored at $\lambda_{Ex} = 360$ nm and $\lambda_{Em} = 480$ nm for samples that incubated or not with (3) and (6) at 10 and 50 μM. Enzymatic activity was recorded in AFU/min (Arbitrary Fluorescence Units per minute) considering 100% activity for the absence of the compound [28]. Assays were carried out in triplicates.

2.10. Data analysis

All tests were performed in triplicates and results were tested statistically compared to the control group. The results were presented as means ± standard deviation and were analyzed using *GraphPad Prism6* software, USA. Ordinary One Way ANOVA was applied comparing treated with untreated control groups. p values <0.05 were considered statistically significant.

3. Results and discussion

3.1. Selection of gold(I)-N-heterocyclic carbenes

The series of symmetric gold(I)-aryl-N-heterocyclic carbenes and gold(I)-benzyl-N-heterocyclic carbenes was selected for a systematic study of the leishmanicidal activity of this class of compounds (Fig. 1). Bulky and electron donating substituents adjacent to the carbene carbon promote kinetic stabilization of M-NHC bond and for this purpose these symmetric carbenes were selected [13]. Two novel structures were prepared (5) and (6). They were characterized by ^{1}H NMR and mass spectrometry. No single crystals were obtained for the compounds. The series are soluble in acetonitrile, DMSO, DMF and chloroform and the spectra of the compounds can be found in Supplementary material (Fig. S1-S30). The replacement of chloride by dimethylaminopyridine (DMAP) adds charge to the complex and increases solubility in polar solvents. Also, the planar nature of DMAP improves the ability of interaction with aromatic protein residues such as tryptophan and phenylalanine, as previously reported by our research group for $[Ph_3PAuDMAP]^+$ derivatives [17]. This is key for the interaction with proteins such as cysteine proteases and zinc fingers.

3.2. In vitro activity of gold(I)-aryl-N-heterocyclic carbenes and gold(I)-benzyl-N-heterocyclic carbenes against Leishmania promastigotes, macrophages and intracellular amastigotes

Next, *L. amazonensis* and *L. braziliensis* logarithmic phase promastigotes were incubated with 100, 50, 25, 12.5, 6.3, 3.1, 1.6 and 0.8 μM of six gold benzyl and aryl-N-heterocyclic carbenes (1)–(6) for 24 h. Effective concentrations capable of inhibiting 50% of parasite (EC_{50}) viability are presented in Table 1. Fifty % cytotoxic concentrations (CC_{50}) for murine bone marrow-derived macrophages (BMDM) were established and ranged from 18.52 to 24.35 μM, allowing us to establish the selectivity index for each compound ($SI = CC_{50}/ EC_{50}$). Au(I)-NHC (3) presented the best SI in the series, followed by (4), while compound (1) showed moderate to poor activity being ruled out from further *in vitro* evaluations. Sensitivity ranges varied minimally between *Leishmania* species, with being (2) slightly more active against *L. amazonensis* (Table 1). This uniform response leads us to speculate that the activity of (2)–(6) is possibly related to conserved targets for both species.

Our systematic study offers the possibility to evaluate structure/activity relationships of this gold(I) symmetric benzyl and aryl-NHC series. By comparing the EC_{50} of (1) and (6), we observe a significant decrease (close to 4.1- and 3,4-fold for *L. amazonensis* and *L. braziliensis*, respectively) when chloride is replaced by DMAP (Table 1), suggesting that the

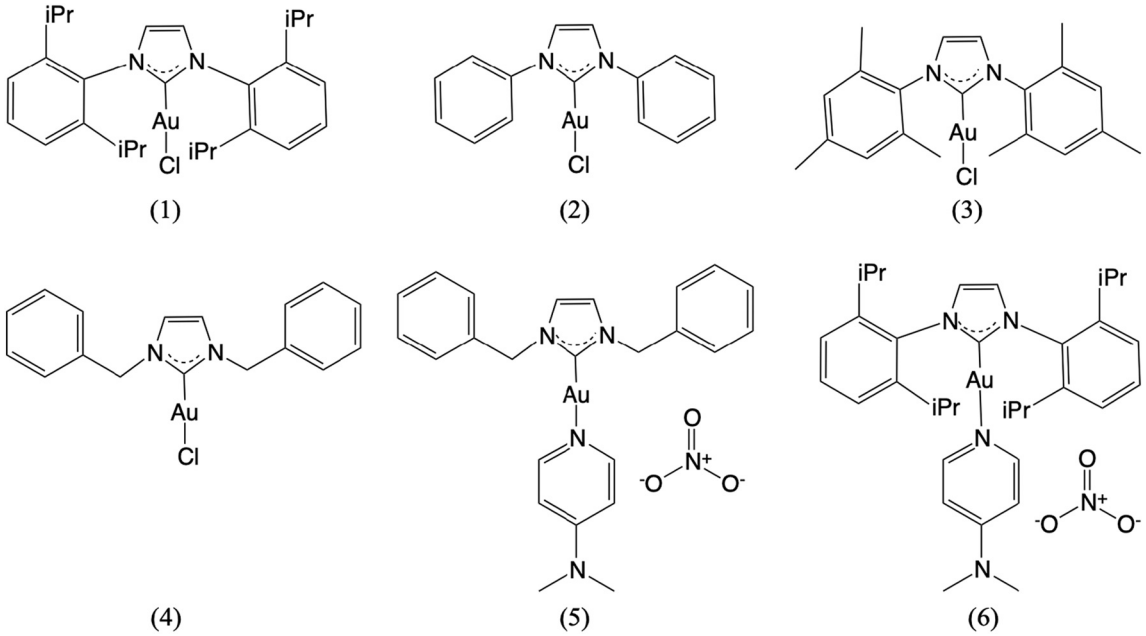

Fig. 1. Structural formulas of the compounds evaluated in this study, iPr = isopropyl group.

Table 1
Antileishmanial activity and cytotoxicity of compounds (1)–(6) after 24 h.

	EC_{50} (μM)[1]		CC_{50} (μM)[2]	Selectivity index	
	Promastigotes		Macrophages		
	L. amazonensis	*L. braziliensis*	BMDM	*L. amazonensis*	*L. braziliensis*
(1)	25.99 ± 4.61	27.83 ± 4.22	nd	nd	nd
(2)	2.11 ± 1.11	8.30 ± 0.88	21.65 ± 0.96	10.3	2.6
(3)	1.57 ± 0.41	1.68 ± 0.36	21.81 ± 1.07	13.9	12.9
(4)	1.65 ± 0.16	1.70 ± 0.42	18.52 ± 1.08	11.2	10.9
(5)	1.96 ± 0.66	2.41 ± 1.62	21.23 ± 1.59	10.8	8.8
(6)	6.35 ± 3.72	8.14 ± 1.79	24.35 ± 1.81	3.8	2.9

[1]Means of EC50: Effective concentration for 50% of promastigotes ± standard deviation and [2] Means of CC50: Cytotoxicity concentration for 50% of BMDM ± standard deviation. Selectivity index = CC_{50}/EC_{50}. Viability assay using MTT was performed as described in the 'Experimental Section'.

relative lower solubility of (1) in polar solvents is perhaps impacting its leishmanicidal effect leading to a higher EC_{50}. In parallel, the comparison of (2), (3) and (4) SIs values suggests a progressive decrease of EC_{50} by the increase of steric hindrance of substituent groups which is reported to have a significant impact in the stability of metal N-heterocyclic-carbenes in solution [29]. The presence of donating methyl groups in position 1,3,5 in the mesityl group of compound (3) could explain its promising result (SI > 13; Table 1) due to the improvement in solution stability [29]. Differentiation between (4) and (5), however, demonstrates that the replacement of chloride by DMAP in [Au(*IBn*)X] does not improve the leishmanicidal activity in a significant manner. None of the basic structural changes seems to have interfered with the cytotoxic activity against BMDM, as sensitivity remained similar with all tested compounds varying from 18.52 to 24.35 μM CC_{50}.

Al-Majid and collaborators tested the activity of cationic gold(I)-bis-NHC. Their results showed good activity of $[Au(iPr)_2]^+$ against *L. major* promastigotes (EC_{50} = 8.2 ± 0.24 μM) in the same micromolar range observed in our study, despite its more pronounced cytotoxicity against 3T3-L1 fibroblasts (CC_{50} = 8.85 ± 0.25 μM) in comparison with PC-3, Hela and MCF-7 neoplastic cell lines [30]. Yet, the choice of fibroblasts and cancer cells for the cytotoxicity assay should not be assumed as the only options when investigating antileishmanial candidates as they are not primary host cells for the parasite [11].

Paloque et al. have synthesized and demonstrated the biological activity of new mononuclear cationic or neutral Au(I) complexes containing quinoline functionalized N-heterocyclic carbenes against *L. infantum* promastigotes and amastigotes and J774A.1 macrophages. The best candidate that showed a SI of 6.19 was the only neutral complex in the series [31]. Zhang et al. explored a series of neutral Au(I)-NHC against *L. infantum* showing the leishmanicidal activity for 50% of promastigote cultures of up to 10 μM for the majority of the complexes with SI ~ 3.0 [32].

There is a limited number of studies in the literature that report morphological alterations in *Leishmania* promastigotes induced by metallic compounds. In this sense, we have examined several images of Giemsa-stained parasites after 24 h incubation with Au(I)-NHC in order to identify possible structural changes on the typical promastigote form (Fig. 2). Increasing concentrations of (2)–(6) were tested and

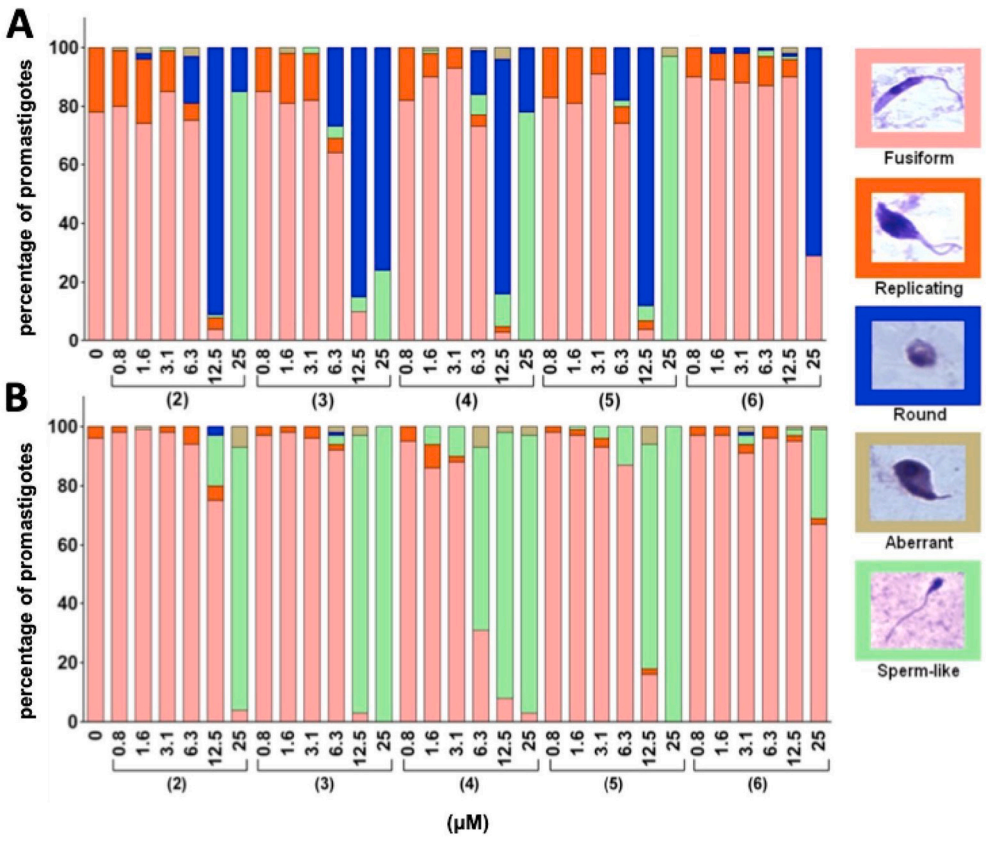

Fig. 2. Quantification of the morphological aspects of *L. amazonensis* (A) and *L. braziliensis* (B) promastigotes (in percentages) observed after 24 h of incubation with 0.8; 1.6; 3.1; 6.3; 12.5 and 25 μM of (2)–(6). Photomicrographs of stained parasites are shown in the right column to exemplify 5 morphotypes detected: *Fusiform*, *Replicating*, *Round*, *Aberrant*, and *Sperm-like*. The color for each image corresponds to the frequency of colored bars in the graph. At least 150 promastigotes were counted for each condition. "0" in the x-axis corresponds to untreated control promastigotes.

promastigotes classified according to the frequency of the shapes detected, being the 'fusiform' and 'replicating' events considered typical for untreated control cells and 'round', 'aberrant' and 'sperm-like' assumed as atypical forms.

Around 10 to 25% of the *L. amazonensis* promastigote population presented detectable morphological changes (round shape without visible flagellum) when incubated with 6.3 μM of (2)–(5) (Fig. 2A). Also, these compounds altered promastigote aspects in a more pronounced way at 12.5 μM with 75–90% of round cells. About 5–10% promastigotes presented the atypical "sperm-like" aspect. At the highest concentration, 100% of cells treated with (2)–(5) showed morphological anomalies. Curiously, compound (6) led to ovoid-shape transformation of parasites (~70%), without more drastic changes such as 'sperm-like' promastigotes at 25 μM seen for (2)–(5), a fact that may reflect its lower leishmanicidal activity (Table 1).

On the other hand, *L. braziliensis* showed lower percentages of dividing cells, both in control and NHC-incubated groups (Fig. 2B). In general, morphological patterns between species were similar, but some differences can be pointed out with (2) at 12.5 μM, for example, that led to less than 20% of *L. braziliensis* altered cells, a finding that may reflect lower sensitivity of this species in the cell viability assay (Table 1). However, (6) proved to be equally less efficient against *L. braziliensis*, inducing abnormal morphology only in ~30% of the cells at the highest concentration.

Lorete-Terra and colleagues detected changes in shape and size of the cell body of *L. amazonensis* promastigotes, such as the occurrence of duplicate flagellum, invagination, rounding and aberrations in the cell body of the parasite when treated with Co(II) complexes [33]. Another study also demonstrated that *L. amazonensis* promastigotes showed a rounding cell body with "sperm-like" aspect upon 10 μM Auranofin exposure, suggesting that this gold-based drug is an inducer of apoptotic-like event in L. *amazonensis* promastigotes [34]. In fact, apoptosis-like cell death in *Leishmania* includes the cascade of several morphophysiological modifications, including cell rounding and shrinkage, changes in plasma membrane despite the maintenance of its integrity, mitochondrial alterations, chromatin condensation, and nuclear and DNA fragmentation [35].

After establishing the effects of our Au(I) complexes against promastigotes, we evaluated the ability of (2)–(6) to inhibit intracellular amastigotes in murine macrophages, relevant stages in the context of leishmaniasis. Fig. 3 shows the results of Au(I)-NHC-treated infections of BMDM with amastigotes assessed by the following parameters: infection rate (Fig. 3A), number of parasites per host cell (Fig. 3B), infectivity index (Fig. 3C) and the absolute number of amastigotes (Fig. 3D). Incubation with (2), (3) and (4) led to a more pronounced reduction of the infection rates and infectivity indexes for *L. amazonensis*, similar to our assays using promastigotes. Compound (3) showed to be the best complex of this systematic series at the lowest concentration (5 μM), being able to reduce the infectivity index by 60% for *L. amazonensis* and ~ 40% for *L. braziliensis*. It is reasonable to speculate that differences observed between the activity against promastigotes and amastigotes may be related to the greater difficulty for molecules to access the parasitophorous vacuole in the interior of host cells, in addition to possible interactions that the complexes suffer with components of the culture media. Chaves et al. also pointed to the involvement of host cell-dependent mechanisms related to the action of the tested molecules, as they initially depend on the uptake/transport across the cell membrane and the parasitophorous vacuole to target intracellular

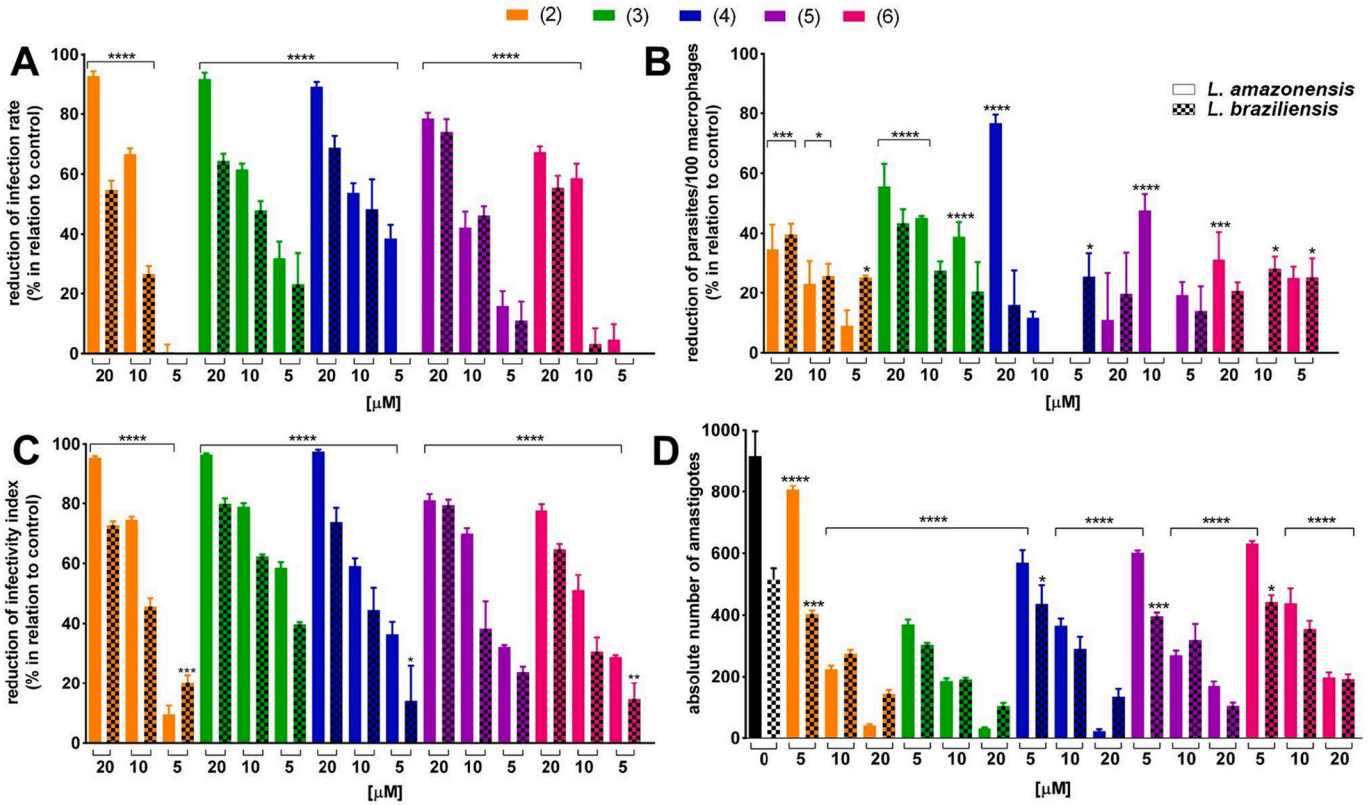

Fig. 3. BMDM infected with promastigotes of *L. amazonensis* at a ratio of 5:1 and *L. braziliensis* (10:1) and incubated with (2)–(6). Each bar refers to the percentage of reduction of the infection rate (A), parasite burden per macrophage (B) and infectivity index (C) in relation to untreated control infections (100%). (D): absolute number of amastigotes counted for the same fields examined for the infection rate and intracellular parasite burden. The results presented are representative of two independent assays performed in triplicate. Ordinary One Way ANOVA was applied as a statistical test comparing treated groups with the untreated control: * $p < 0.05$; ** $p < 0.01$; ***$p < 0.001$; **** $p < 0.0001$.

amastigotes [36]. Even so, we have included the quantification of the absolute number of amastigotes in order to show that concentrations capable of inhibiting 50% of the intracellular parasite burden remained below 10 μM for (2) and (3), especially for *L. amazonensis* (Fig. 3D), highlighting that these candidates show very good antileishmanial activity.

3.3. Plasma membrane interference induced by (3)

Due to the morphological changes (Fig. 2) and amastigote sensitivity characterized upon exposure to Au(I) complexes, mainly (3) against *L. amazonensis*, our next step was to determine whether (3) could be interfering with the permeability of the plasma membrane of *L. amazonensis*. In this case, promastigotes and axenic amastigotes were examined regarding possible effects on cell plasma membrane permeabilization after incubation with (3) at 0.78 μM (half- EC_{50}) and 1.57 μM (EC_{50}) for 15 and 25 min (short time point) and 24 h (long time point) followed by EtBr exposure (Fig. 4). For promastigotes, compound (3) at the EC_{50} increased cell membrane permeability in 30% and 50% (compared to untreated parasites) after 15 and 25 min of incubation, respectively (Fig. 4A). After 24 h of incubation, a 20% and 86% increase in plasma membrane permeability was observed after incubation with half- EC_{50} and EC_{50}, respectively (Fig. 4B). For amastigotes, ~ 9% and 16% increase was observed after 15 min and 24 h, respectively, of incubation with EC_{50} (Fig. 4C). Our results suggest that initial exposure of the parasites at low concentration of (3) is sufficient to disturb cell organization.

Recently, Minori et al. showed an increase in membrane permeability of *L. amazonensis* promastigotes and axenic amastigotes incubated with Au(I) and Au(III) compounds, the most effective being an Au (III) complex coordinated to a bidentate NˆN scaffold, which caused a ~ 50% increase in permeability of promastigotes after 3 h. In general, all compounds were effective in destabilizing membrane permeability. Higher influxes of EtBr and similar results between 3 and 24 h of incubation were also detected for amastigotes [14]. Moreover, Sharlow et al. demonstrated that *L. amazonensis* promastigotes became round after 5 h of Auranofin exposure. The authors argue that this phenotype can be attributed to trypanothione reductase inhibition and increased membrane permeability, which lead to an apoptosis-like response. They also reported an increase in caspase 3/7-like activity and DNA fragmentation after exposure to Auranofin [34].

3.4. Inhibition of recombinant cysteine proteases by (3) and (6)

Cysteine proteases (CP) are found in different species of *Leishmania*, being essential for

parasite infectivity, evasion of the immune system, promastigote to amastigote transformation and nutrition. There are three classes of CP in *L. mexicana* known as CPA and CPB, both cathepsin-L-like, and CPC, a cathepsin-B-like [28,37,38]. The CPB gene comprises 14 copies and the CPB2.8 enzyme is stage-regulated and the most abundant of them. It contains Asn-60, Asp-61 and Asp-64 located in an α-helix, which is part of the wall of the catalytic site. The CPB3.0 enzyme has the variant residues Asp-60, Asn-61 and Ser-64. CPB18 contains Asp-60, Asn-61 and Ser-64 and also Try-84 and Asn-18 instead of His-84 and Asp-18, respectively in CPB2.8 [39]. These variations in positions 60, 61, 64 and 84 between CPB2.8 and isoforms alter charge distribution causing significant changes in the electrostatic potential on the surface of isoenzymes. The mutated version rH84Y has His-84 replaced by Tyr-84, in an attempt to mimic the structure of CPB18, but keeping the Asp-18 instead of Asn-18; interfering with the binding of molecules possibly thus changing the geometry of the catalytic site [37,40].

Knowledge in parasite biology has shown the involvement of enzymes in the replication, survival, and pathogenicity of *Leishmania* and *Trypanosoma* species. In this context, CP have been shown to be promising targets for drug discovery of antiprotozoal drugs [41]. As it is well established in the literature that metal complexes are potent inhibitors of *Leishmania* CP [8,42], we chose to evaluate whether the most and least active compounds against amastigote forms ((3) and (6), respectively) would be able to directly inhibit rCPB2.8, rCPB3.0 and rH84Y

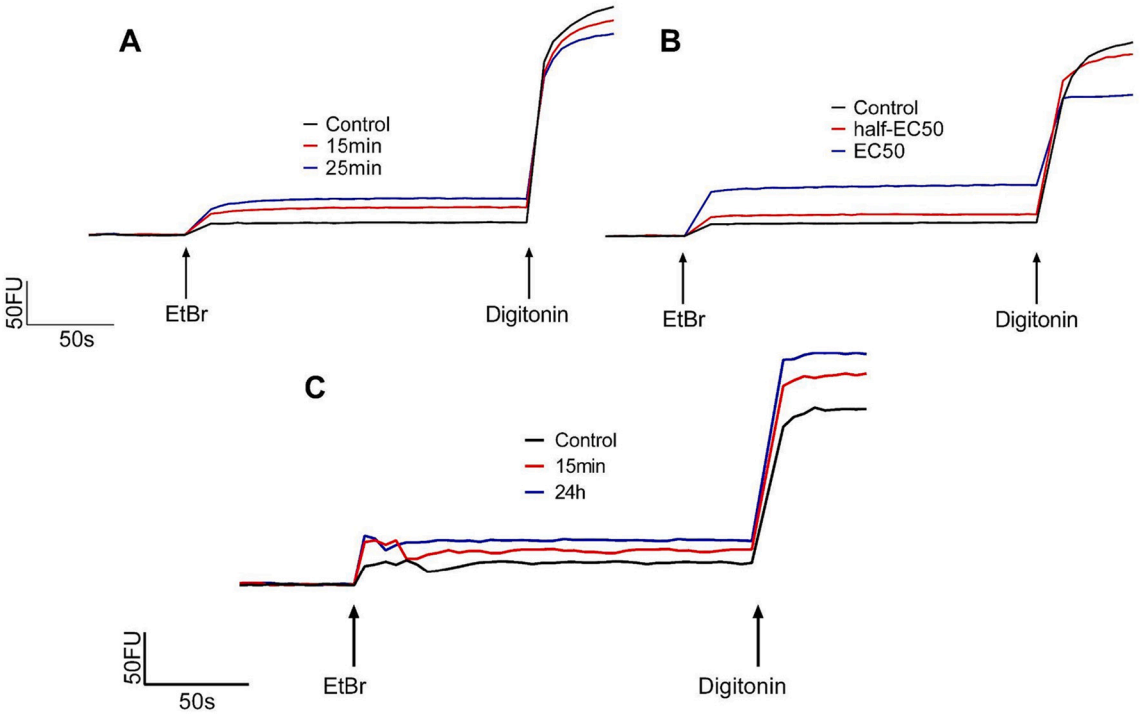

Fig. 4. *L. amazonensis* plasma membrane permeability assay after incubation with (3). (A) 5×10^6 promastigotes were incubated for 15 and 25 min with (3) EC_{50} and (B) 24 h with half-EC_{50} and EC_{50} of (3). (C) 1×10^7 amastigotes were incubated for 15 min and 24 h with the EC_{50} of (3). Arrows show addition of ethidium bromide (EtBr) and digitonin. Scale bar shows fluorescence units (FU) by time (seconds).

activities at the mammalian host temperature (Fig. 5). The advantage of using recombinant *L. mexicana* enzymes relies on the fact that results can be easily extrapolated to *L. amazonensis*, extensively explored in our study, since the latter is a species that belongs to the mexicana complex [43].

The rCPB2.8 activity was more affected by compound (6) than (3) essentially at the lower dose. In contrast, rCPB3.0 variant responded similarly to (3) and (6) at 50 μM, while the mutated version rH84Y showed less sensitivity to both compounds, despite their residual activities having been reduced significantly especially at the highest concentration. Metal complexes can inhibit these enzymes *via* a ligand substitution with the thiol of the active site cysteine [44]. In this way, the cyclopalladate complex [Pd(C2,N-DMPA)(DPPE)] is able to destroy *L. amazonensis in vitro* and by intralesional administration *in vivo* and to inhibit CP cathepsin-like at micromolar concentration [8]. Studies of Massai et al. [42] showed that a series of Au(I) and Au(III) complexes with a variety of ligands, including [Au(*NHC*)Cl], for which NHC is 1-butyl-3-methyl-2,3-dihydro-1H-imidazol-2-ylidene, were found to strongly inhibit human cathepsins (B and L) as well as *L. mexicana* rCPB2.8.

Substitution of negative charges (Asp) at positions 61 and 64 of rCPB2.8 by Asn-61 and Ser-64 in rCPB3.0 was able to reduce the effectiveness of compounds (3) and (6) indicating that electrostatic interactions promoted by residues 61 and 64 are important in the compound enzyme interaction. Metal complex such as Au(I) could inhibit CP by ligand exchange with the thiol of active site because the reduced pK a of reactive Cys favors the interaction of thiophilic metal since gold has high affinity for thiolates with a low pKa [44]. Since the substitution of residues 60, 61 and 64 of rCB2.8 modify the pKa values of CPB enzymes [39], it could imply changes in the interactions of Au(I) compounds as observed in Fig. 5. Interestingly, it is observed that the mutation at position 84 with substitution of His (positive charge) by Tyr (hydrophobic) further reduced the inhibitory effectiveness of rH84Y by both compounds. His-84 is located in an outer loop on the surface of the enzyme and positioned near the Cys56-Cys101 disulfide bridge [40]. Perhaps, its substitution by Tyr may interfere in the structural function of Cys-56 – Cys-101 leading to structural changes to amino acids with important roles in the catalytic site such as Ser-61, Gly-65, Gly-66, Leu-67 and Met-68 (S2/S3 subsite residues) and consequently interfering in the binding of the compounds.

4. Conclusions

Symmetric Au(I) benzyl and aryl-NHC are stable molecules that are easily synthesized. From our series, with the exception of (1), all Au(I)-NHC complexes tested induced a concentration-dependent antiproliferative effect on promastigotes. The series allowed the investigation of the effects of N-substituents against two relevant *Leishmania* species. The bulkiest 2,4-diisopropylphenyl (1) substituent showed the lowest SI, followed by the phenyl derivative (2). Replacing chloride by DMAP slightly improved the SI for the 2,4-diisopropylphenyl derivative (6), suggesting that lipophilicity is playing a role in the effectiveness of these compounds. The best results found for (3) indicate that a balance of steric hindrance and electronic parameters of the NHC are significant. At sublethal concentrations, parasites showed substantial morphological changes. In mechanistic evaluations of the best candidate (3), the increased membrane permeability and inhibition of CP enzymatic activity, which make up an extremely relevant arsenal of signaling molecules of the parasite, point to possible targets that may explain the specificity of these compounds. In general, all compounds were shown to be active in reducing intracellular infection, with *L. amazonensis* being more sensitive to these compounds. However, (3) should be highlighted as an interesting chemotype for further developments. Our findings pave the way for further experimental treatment schemes with this mesityl derivative alone or in association with drugs used in clinical practice against ATL.

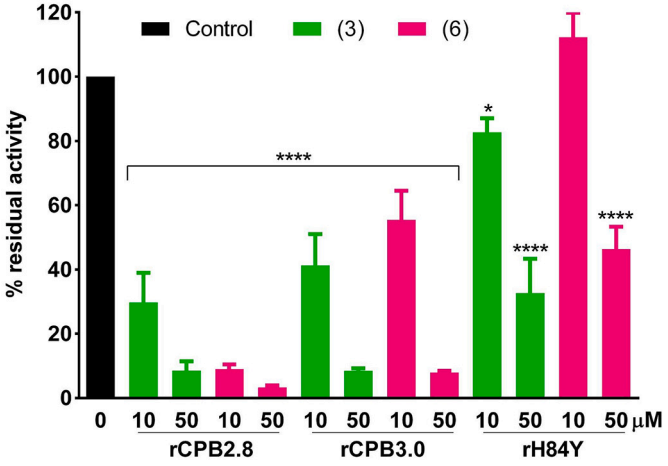

Fig. 5. Percentages of the residual activities of *L. mexicana* rCPB2.8, rCPB3.0 and rH84Y were obtained using *Z*-FR-MCA, a fluorogenic substrate specific for cathepsin B-like proteases, after incubation with (3) and (6) at 10 and 50 μM as described in the 'Experimental Section'. Enzymatic activity was recorded in FAU/min (Fluorescence Arbitrary Units per minute) considering 100% activity for the absence of any compound ("0"). Assay was run in three biological replicates. *$p < 0.05$; ****$p < 0.0001$.

Authorship statement

None.

Declaration of Competing Interest

None.

Acknowledgements

This work was financially supported by São Paulo Research Foundation (FAPESP) (#2014/02205-1, 2016/25112-4 and 2019/01678-7 [WASJ], 2018/21120-8; 2019/16904-2 [CA], 2014/21129-4 [DCM]), Brazilian National for Scientific and Technological Development (CNPq) process# MCTIC/CNPq 28/2018 406444/2018-8 - CA and FAEPEX-PRP/Unicamp (#519.292 - DCM). LBR, RLAL and JVF received CAPES-DS Master scholarships. C.G. received a CNPq scholarship (#142280/2017-8). We thank Dr. Fernanda R. Gadelha for her technical support and Ana J. Vincoletto for the assistance with promastigotes' morphology analysis.

Appendix A. Supplementary data

Supplementary data to this article can be found online at https://doi.org/10.1016/j.jinorgbio.2022.111726.

References

[1] W. H. Organization, Control of Neglected Tropical Diseases. https://www.who.int/teams/control-of-neglected-tropical-diseases/overview, 2021 (accessed January 2022).
[2] D.C. Miguel, M.B.C. Brioschi, L.B. Rosa, K. Minori, N. Grazzia, The impact of COVID-19 on neglected parasitic diseases: what to expect? Trends Parasitol. 37 (2021) 694–697.
[3] E. Torres-Guerrero, M.R. Quintanilla-Cedillo, J. Ruiz-Esmenjaud, R. Arenas, Leishmaniasis: a review, F1000Res 6 (2017) 750.
[4] J. Silva, A. Queiroz, I. Moura, R.S. Sousa, L.H. Guimarães, P.R.L. Machado, M. Lessa, E. Lago, M.E. Wilson, A. Schriefer, Dynamics of American tegumentary leishmaniasis in a highly endemic region for Leishmania (Viannia) braziliensis infection in Northeast Brazil, PLoS Negl. Trop. Dis. 11 (2017), e0006015.
[5] L.M. Alcântara, T.C.S. Ferreira, F.R. Gadelha, D.C. Miguel, Challenges in drug discovery targeting TriTryp diseases with an emphasis on leishmaniasis, Int. J. Parasitol. Drugs Resist. 8 (2018) 430–439.

[6] R.S. Maffei, J.K.U. Yokoyama-Yasunaka, D.C. Miguel, S.R.B. Uliana, B.P. Espósito, Synthesis, characterization and evaluation of antileishmanial activity of copper(II) with fluorinated α-hydroxycarboxylate ligands, Biometals 22 (2009) 1095–10101.
[7] M.S. Costa, Y.G. Gonçalves, S.C. Teixeira, D.C.O. Nunes, D.S. Lopes, C.V. Silva, M. S. Silva, B.C. Borges, M.J.B. Silva, R.S. Rodrigues, V.M. Rodrigues, G.V. Poelhsitz, K.A.G. Yoneyama, Increased ROS generation causes apoptosis-like death: mechanistic insights into the anti-Leishmania activity of a potent ruthenium(II) complex, J. Inorg. Biochem. 195 (2019) 1–12.
[8] C.S. Paladi, I.A.S. Pimentel, S. Katz, R.L.O.R. Cunha, W.A.S. Judice, A.C.F. Caires, C.L. Barbiéri, In vitro and in vivo activity of a Palladacycle complex on Leishmania (Leishmania) amazonensis, PLoS Negl. Trop. Dis. 6 (2012), e1626.
[9] J.M. Méndez-Arriaga, G.M. Esteban-Parra, M.J. Juárez, A. Rodríguez-Diéguez, M. Sánchez-Moreno, J. Isac-García, J.M. Salasa, Antiparasitic activity against trypanosomatid diseases and novel metal complexes derived from the first time characterized 5-phenyl-1,2,4-triazolo[1,5-a]pyrimidi-7(4H)-one, J. Inorg. Biochem. 175 (2017) 217–224.
[10] G.L. Silva, J.S.M. Dias, H.V.R. Silva, J.S. Teixeira, I.R.B. Souza, E.T. Guimarães, D. R.M. Moreira, M.B.P. Soares, M.I.F. Barbosa, A.C. Doriguetto, Synthesis, crystal structure and leishmanicidal activity of new trimethoprim Ru(III), cu(II) and Pt(II) metal complexes, J. Inorg. Biochem. 205 (2020) 111002.
[11] L.B. Rosa, R.L. Aires, L.S. Oliveira, J.V. Fontes, D.C. Miguel, C. Abbehausen, A "Golden Age" for the discovery of new antileishmanial agents: current status of leishmanicidal gold complexes and prospective targets beyond the trypanothione system, ChemMedChem. 16 (2021) 1682–1696.
[12] R. Manhas, V.S. Gowri, R. Madhubala, Leishmania donovani encodes a functional selenocysteinyl-tRNA synthase, J. Biol. Chem. 291 (2015) 1203–1220.
[13] M.N. Hopkinson, C. Richter, M. Schedler, F. Glorius, An overview of N-heterocyclic carbenes, Nature. 510 (2014) 485–496.
[14] K. Minori, L.B. Rosa, R. Bonsignore, A. Casini, D.C. Miguel, Comparing the antileishmanial activity of Gold(I) and Gold(III) compounds in L. amazonensis and *L. braziliensis* in Vitro, ChemMedChem 15 (2020) 2146–2150.
[15] C. Zhang, C. Hemmert, H. Gornitzka, O. Cuvillier, M. Zhang, R.W.-Y. Sun, Cationic and neutral N-heterocyclic carbene gold(I) complexes: cytotoxicity, NCI-60 screening, cellular uptake, inhibition of mammalian thioredoxin reductase, and reactive oxygen species formation, ChemMedChem 13 (2018) 1218–1229.
[16] S. Ftouh, S. Bourgeade-Delmas, M. Belkadi, C. Deraeve, C. Hemmert, A. Valentin, H. Gornitzka, Synthesis, characterization, and antileishmanial activity of neutral gold(I) complexes with N-heterocyclic carbene ligands bearing sulfur- containing side arms, Organometallics. 40 (2021) 1466–1473.
[17] C. Abbehausen, E.J. Peterson, R.E.F. de Paiva, P.P. Corbi, A.L.B. Formiga, Y. Qu, N. P. Farrell, Gold(I)-phosphine-N-heterocycles: biological activity and specific (ligand) interactions on the C-terminal HIVNCp7 zinc finger, Inorg. Chem. 52 (2013) 11280–11287.
[18] W.L.F. Armarego, Chapter 3 - purification of organic chemicals, in: Purification of Laboratory Chemicals, eighth ed., Butterworth-Heinemann, Oxford, 2017, pp. 95–634.
[19] R. Uson, A. Laguna, M. Laguna, D.A. Briggs, H.H. Murray, J.P. Fackler Jr., Chapter 17 - (Tetrahydrothiophene)Gold(I) or Gold(III) Complexes, in: H.D. Kaesz (Ed.), Inorganic Syntheses 26, John Wiley & Sons, Inc, New York, 1989, pp. 85–91.
[20] P. Murer, T. Gessner, C. Eickhoff, J. Birnstock, F. May, K. Kahle, Electroluminescent imidazo-quinoxaline carbene metal complexes, WO2016020516A1, Fev 11 (2016). https://patents.google.com/patent/WO2016020516A1/en.
[21] L.R. Moore, S.M. Cooks, M.S. Anderson, H.-J. Schanz, S.T. Griffin, R.D. Rogers, M. C. Kirk, K.H. Shaughnessy, Synthesis and characterization of water-soluble silver and palladium Imidazol-2-ylidene complexes with noncoordinating anionic substituents, Organometallics 25 (2006) 5151–5158.
[22] M. Hans, J. Lorkowski, A. Demonceau, L. Delaude, Efficient synthetic protocols for the preparation of common N-heterocyclic carbene precursors, Beilstein J. Org. Chem. 11 (2015) 2318–2325.
[23] R. Visbal, A. Laguna, M.C. Gimeno, Simple and efficient synthesis of [MCI(NHC)] (M = au, ag) complexes, Chem. Commun. 49 (2013) 5642–5644.
[24] A. Collado, A. Gómez-Suárez, A.R. Martin, A.M.Z. Slawin, S.P. Nolan, Straightforward synthesis of [au(NHC)X] (NHC = N-heterocyclic carbene, X = cl, Br, I) complexes, Chem. Commun. 49 (2013) 5541–5543.
[25] R.L. Renberg, X. Yuan, T.K. Samuel, D.C. Miguel, I. Hamza, N.W. Andrews, A. R. Flannery, The Heme transport capacity of LHR1 determines the extent of virulence in Leishmania amazonensis, PLoS Negl. Trop. Dis. 9 (2015), e0003804.
[26] D.C. Miguel, A.R. Flannery, B. Mittra, N.W. Andrews, Heme uptake mediated by LHR1 is essential for Leishmania amazonensis virulence, Infect. Immun. 81 (2013) 3620–3626.
[27] P. Kumar, A. Nagarajan, P.D. Uchil, Analysis of cell viability by the MTT assay, Cold Spring Harb. Protoc (2018), https://doi.org/10.1101/pdb.prot095505.
[28] W.A.S. Judice, M.A. Manfredi, G.P. Souza, T.M. Sansevero, P.C. Almeida, C. S. Shida, T.F. Gesteira, L. Juliano, G.D. Westrop, S.J. Sanderson, G.H. Coombs, I.L. S. Tersariol, Heparin modulates the endopeptidase activity of leishmania mexicana cysteine protease cathepsin L-Like rCPB2.8, PLoS ONE 8 (2013) e80153.
[29] H.-L. Su, L.M. Pérez, S.-J. Lee, J.H. Reibenspies, H.S. Bazzi, D.E. Bergbreiter, Studies of ligand exchange in N-heterocyclic carbene silver(I) complexes, Organometallics 31 (2012) 4063–4071.
[30] A.M. Al-Majid, S. Yousuf, M.I. Choudhary, F. Nahra, S.P. Nolan, Gold-NHC complexes as potent bioactive compounds, ChemistrySelect. 1 (2016) 76–80.
[31] L. Paloque, C. Hemmert, A. Valentin, H. Gornitzka, Synthesis, characterization, and antileishmanial activities of gold(I) complexes involving quinolone functionalized N-heterocyclic carbenes, Eur. J. Med. Chem. 94 (2015) 22–29.
[32] C. Zhang, S.B. Delmas, Á.F. Álvarez, A. Valentin, C. Hemmert, H. Gornitzka, Synthesis, characterization, and antileishmanial activity of neutral N-heterocyclic carbenes gold(I) complexes, Eur. J. Med. Chem. 143 (2018) 1635–1643.
[33] A. Lorete-Terra, J.M. Tostes, R.A. da Matta, C.B. de Santana Filho, C. Fernandes, A. H. Junior, F.S. de Azevedo Fortes, S.H. Seabra, In vitro activity on Leishmania amazonensis promastigote forms of a new Co(II) coordination complex, Braz. J. Dev. 7 (2021) 14653–14668.
[34] E.R. Sharlow, S. Leimgruber, S. Murray, A. Lira, R.J. Sciotti, M. Hickman, T. Hudson, S. Leed, D. Caridha, A.M. Barrios, D. Close, M. Grögl, A.S. Lazo, Auranofin is an apoptosis-simulating agent with in vitro and in vivo anti-leishmanial activity, ACS Chem. Biol. 9 (2014) 663–672.
[35] L. Basmaciyan, M. Casanova, Cell death in Leishmania, Parasite 26 (2019) 1–13.
[36] J.D.S. Chaves, L.G. Tunes, C.H.J. Franco, T.M. Francisco, C.C. Corrêa, S.M. F. Murta, R.L. Monte-Neto, H. Silva, A.P.S. Fontes, M.V. de Almeida, Novel gold(I) complexes with 5-phenyl-1,3,4-oxadiazole-2-thione and phosphine as potential anticancer and antileishmanial agents, Eur. J. Med. Chem. 127 (2017) 727–739.
[37] J.C. Mottram, M.J. Frame, D.R. Brooks, L. Tetley, J.E. Hutchison, A.E. Souza, G. H. Coombs, The multiple cpb cysteine proteinase genes of Leishmania Mexicana encode isoenzymes that differ in their stage regulation and substrate preferences, J. Biol. Chem. 272 (1997) 14285–14293.
[38] H. Azizi, K. Hassani, Y. Taslimi, H.S. Najafabadi, B. Papadopoulou, S. Rafati, Searching for virulence factors in the non-pathogenic parasite to humans Leishmania tarentolae, Parasitology. 136 (2009) 723–735.
[39] W.A.S. Judice, J.C. Mottram, G.H. Coombs, M.A. Juliano, L. Juliano, Specific negative charges in cysteine protease isoforms of Leishmania mexicana are highly influential on the substrate binding and hydrolysis, Mol. Biochem. Parasitol. 144 (2005) 36–43.
[40] M.A. Juliano, D.R. Brooks, P.M. Selzer, H.L. Pandolfo, W.A.S. Judice, L. Juliano, M. Meldal, S.J. Sanderson, J.C. Mottram, G.H. Coombs, Differences in substrate specificities between cysteine protease CPB isoforms of Leishmania mexicana are mediated by a few amino acid changes, Eur. J. Biochem. 271 (2004) 3704–3714.
[41] W.A.S. Judice, L.S. Ferraz, R.M. Lopes, L.S. Vianna, F.S. Siqueira, J.F.D. Iorio, L.A. M. Dalzoto, M.N.R. Trujilho, T.R. Santos, M.F.M. Machado, T. Rodrigues, Cysteine proteases as potential targets for anti-trypanosomatid drug discovery, Bioorg. Med. Chem. 46 (2021) 116365.
[42] L. Massai, L. Messori, N. Micale, T. Schirmeister, L. Maes, D. Fregona, M.A. Cinellu, C. Gabbiani, Gold compounds as cysteine protease inhibitors: perspectives for pharmaceutical application as antiparasitic agents, Biometals. 30 (2017) 313–320.
[43] K. Vickerman, The diversity of the kinetoplastid flagellates, in: W.H.R. Lumsden, D. A. Evans (Eds.), Biology of the kinetoplastida, Academic Press, London, 1976, pp. 1–34.
[44] S.P. Fricker, Cysteine proteases as targets for metal-based drugs, Metallomics. 2 (2010) 366–377.